Polymeric Micelles with Glycolipid-like Structure and Multiple Hydrophobic Domains for Mediating Molecular Target Delivery of Paclitaxel

Jian You, Fu-Qiang Hu,* Yong-Zhong Du, and Hong Yuan

College of Pharmaceutical Sciences, Zhejiang University, Yuhangtang Road 388, Hangzhou 310058, People's Republic of China

Received April 3, 2007; Revised Manuscript Received June 15, 2007

Herein, polymeric micelles with glycolipid-like structure and about 40 nm diameter are prepared by self-aggregation from stearate-grafted chitosan oligosaccharides in aqueous medium. The micelles, with high degree of substitution (DS), present specific spatial structure with multiple hydrophobic "minor cores", and thus obtain excellent internalization into cancer cells and accumulation in cytoplasm. Furthermore, the micelles showed pH-sensitive properties, thus favoring intracellular delivery of encapsulated drug via endocytosis. The cell cytotoxicity of paclitaxel encapsulated in micelles was improved sharply and contributed to the increased intracellular delivery of the drug. The present micelles are a promising carrier candidate for targeting therapy of antitumor drugs with a cytoplasmic molecule target.

1. Introduction

To improve antitumor efficacy and minimize undesired drug toxicity toward healthy tissues, the usual strategy is to design drug delivery systems to have targeted accumulation of drug at the tumor site. As a result of the enhanced permeability and retention (EPR) effect,[1] passive targeting results in the selective extravasation and accumulation of drug carriers in tumor tissues.[2] Furthermore, the drug carriers can attain active targeting, which is expected to lead to higher intratumoral accumulation, by being derivatized with ligands that bind to specific receptors expressed on target cells.[3] However, for a variety of anticancer drugs with an intracellular action site, the accumulation of these drugs in tumor tissues is not a guarantee of sharp therapeutic improvement. Efficient internalization of antitumor drug into cancer cells and accumulation at its intracellular molecular target should be the determinant steps for the antitumor activity. The main barrier for internalization of drugs or carriers into cells is the cellular membrane. Over the past decade, many approaches have been proposed to overcome the celluar membrane limitations and thus obtain enhanced intracellular delivery of therapeutic agents, including electroporation,[4] viral delivery systems,[5] liposomes,[6,7] encapsulation in polymers,[8] and receptor-mediated endocytosis.[9] Unfortunately, these approaches are often plagued with limited efficiency or cause appreciable cellular toxicity.

Block copolymer micelles are typically spherical, nanosized (10−100 nm) supramolecular assemblies of amphiphilic copolymers.[8] The core of these micelles is a loading space that accommodates hydrophobic drugs, and the hydrophilic outer shell facilitates dispersal of the micelles in water. Polymeric micelles were often employed as promising drug carriers.[10−12] However, the conventional polymeric micelles are usually composed of hydrophobic segments as the internal core and hydrophilic segments as a surrounding corona in aqueous medium. Even if the micelles may possess smaller size compared with other carriers, such as liposomes (50−150 nm) and polymeric nanoparticles (10−1000 nm),[13] the hydrophilic segments on the micelle surface may disfavor micellar internalization into cells because of the lipophilicity of the cellular membrane.

Polysaccharide is a key component unit of the receptor on the cellular membrane, which plays important roles in transmembrane transport.[14] Chitosan and its derivatives are widely accepted for use as drug carriers.[15−17] It was found that the deoxycholic acid-modified chitosan could self-aggregate with several hydrophobic domains.[18] Lipid is compatible with the cellular membrane, which is often confirmed to promote the cellular uptake of encapsulated drug.[19,20] Presumably, the combination of the lipid and polysaccharide can form a novel polymer micelle in aqueous medium. The hydrophobicity of the micelle surface should be enhanced if the micelle can form several hydrophobic domains and some of these domains locate on the micelle surface. As a result, the micelles possess possibly great membrane permeability and rapid intracellular uptake, contributing to their special spatial structure and components.

In previous research,[21,22] the novel self-aggregate of stearate-grafted chitosan oligosaccharide (CSSA), which was synthesized by a coupling reaction between the amino groups of chitosan oligosaccharide and carboxyl group of stearic acid, was used to control the release of paclitaxel (PTX)[21] and as an efficient gene vector.[22] Herein, we synthesized a micelle with higher degree of substitution (DS), which presented excellent internalization into cancer cells and ability to accumulate in cytoplasm. The micelles were used as a carrier to encapsulate PTX to improve the antitumor activity of PTX by transporting the drug into its molecular target site. The drug, PTX, has demonstrated significant activity in clinical trials against a variety of tumors, with the mechanism of action involving the ability to promote polymerization of tubulin dimers in cytoplasm to form microtubules and stabilize the microtubules by preventing depolymerization.[23−25]

* Author to whom correspondence should be addressed. Phone: 086-751-88206742. Fax: 086-751-88206742. E-mail: hufq@zju.edu.cn.

10.1021/bm070365c CCC: $37.00
Published on Web 07/28/2007

2. Materials and Methods

Chitosan was supplied by Yuhuan Marine Biochemistry Co., Ltd. (Zhejiang, China); stearic acid was from Shanghai Chemical Reagent Co. Ltd. (China); 1-ethyl-3-(3-dimethylaminopropyl)carbodiimide (EDC) and 2,4,6-trinitrobenzenesulfonic acid (TNBS) were from Sigma (St. Louis, MO); PTX was purchased from Zhanwang Biochemical Co., Ltd. (Huzhou, China); pyrene was purchased from Aldrich Chemical Co.; 1-dodecylpyridinium (DPC) was purchased from Aldrich Co. and purified by double recrystallization from absolute ethanol; 3-[4,5-dimethylthiazol-2-yl]-2,5-diphenyltetrazolium bromide (MTT) was purchased from Sigma (St. Louis, MO). All other solvents and reagents were used as chemical grade.

Synthesis of Chitosan Oligosaccharide−Stearic Acid Graft Polymer. Chitosan oligosaccharide (M_w = 34 000, degree of deacetylation = 95%) was prepared according to the previous study.[21] CSSA was synthesized via reaction of the carboxyl group of stearic acid with the amine group of chitosan oligosaccharide in the presence of EDC. Briefly, chitosan oligosaccharide (2.0 g) was dissolved in 50 mL of distilled water. Stearic acid (1.75 g) and EDC (10 mol/mol of stearic acid) were dissolved in 40 mL of ethanol. Chitosan oligosaccharide solution was heated to 80 °C under vigorous stirring accompanied by dropwise addition of stearic acid solution. The reaction lasted 5 h. The byproducts were removed via ultrafiltration by Millipore Labscale TFF system [molecular weight cutoff (MWCO) 10 000]. The obtained product was lyophilized (Labconco, FreeZone 2.5 Plus), further washed with ethanol, and separated by the centrifugation (3K30, Sigma Labrorzentrifugen GmbH). The result product was dried in a vacuum oven at 50 °C. The degree of substitution (DS), defined as the number of stearic acid groups per 100 anhydroglucose units of chitosan, was determined by the TNBS method.[26]

^{1}H NMR Measurements. ^{1}H NMR spectra were acquired on a NMR spectrometer (AC-80, Bruker Biospin, Germany) in D_2O at pH 7 and 25 °C.

Particle Size and ζ Potential. Average particle diameter, size distribution, and ζ potential of drug-free micelles and PTX-loaded micelles in aqueous media with different pH (6.2 and 7.4) were measured by dynamic light scattering using a Zetasizer (3000HS, Malvern Instruments Ltd.).

Atomic Force Microsopic Measurement. Samples for atomic force microscopic (AFM) imaging were prepared by depositing 5 μL of an aqueous dispersion of micelles (ca. 0.2 mg/mL) onto the mica surface (APS-mica) for 10 min, and then drying under argon atmosphere. The AFM imaging was visualized (SPA3800N, Seiko) in tapping mode, using high resonant frequency (F_0 = 129 kHz) pyramidal cantilevers with silicon probes having force constants of 20 N/m. Scan speeds were set at 2 Hz. Images were processed and the widths of the particles were measured by use ofSPIWin version 3.0 software.

Critical Aggregation Concentration Measurements. For the determination of intensity ratio of the first to the third highest energy bands in the pyrene emission spectra, the sample solution containing pyrene (6.0×10^{-7} mol/L) was excited at 337 nm, and the emission spectra were recorded in the range of 350−450 nm at 10 nm/min scan rate. The slit openings for excitation and emission were at 10.0 and 2.5 nm, respectively. The spectra were accumulated with an integration time of 5 s/nm.

PTX-Loaded Micelles. PTX-loaded micelles were prepared by dialysis, acording to the reported literature.[27] Briefly, the micelles (20 mg) was dissolved in 5 mL of water/DMSO (1:9) containing PTX and stirred for 3 h at room temperature, followed by dialysis against pure water (Milli-Q, Millipore) overnight at room temperature with a dialysis membrane (MWCO 7000). Then the solution containing the micelles and PTX was centrifuged at 5000 rpm for 5 min. The supernatant was filtered with a 0.22 mm pore-sized microfiltration membrane and, then, was lyophilized.

Measurement of PTX Concentration in CSSA Micellar Solution. The concentration of PTX in the micellar solution was determined by high-performance liquid chromatography (LC-6A, Waters). The mobile phase was a mixture of acetonitrile and water (50:50 v/v). The column was a Symmetry C_{18} (3.9 × 150 mm) with 5 μm particles. The flow rate was 1.0 mL/min, the detection wavelength was 227 nm, and the column temperature was 30 °C. Injected volume of the sample was 20 μL.

PTX Release from Micelles. In vitro cumulative release of PTX from the micelles was investigated in the dissolution medium containing 1 M sodium salicylate with different pH (6.2 and 7.4, adjusted by 0.1 N HCl or 0.1 N NaOH).[28] The freeze-dried PTX-loaded micelles were weighed, dissolved in 1 mL of distilled water, and introduced into a dialysis membrane bag (MWCO = 6000−8000, Spectrum Lab., Rancho Dominguez, CA). The release experiment was initiated by placing the end-sealed dialysis bag in 20 mL of medium at 37 °C. The release medium was stirred at a speed of 100 rpm. At various time points, the medium was refreshed. Samples were taken a predetermined times from the medium outside the dialysis, and their PTX concentrations were determined by HPLC, as described above.

As a control, the drug diffusion of free PTX, which was prepared by dissolving PTX in a 50:50 mixture of Cremophor EL and dehydrated alcohol, from dialysis bag was conducted under the same conditions.

In Vitro Cytotoxicity Assay. HeLa (cervical carcinoma) and A549 (lung carcinoma) cell lines were obtained from Cell Resource Center of China Science Academy and were maintained in DMEM (Dulbecco's modified Eagle's medium) containing 10% fetal bovine serum, 100 units/mL penicillin, and 100 μg/mL streptomycin. Cells were cultured with complete medium at 37 °C in a humidified atmosphere of 5% CO_2 in air. For all of the experiments, cells were harvested from subconfluent cultures by use of trypsin and were resuspended in fresh complete medium before plating.

A comparison of in vitro cytotoxicity of free PTX and PTX-loaded micelles was performed on A549 and HeLa cells with an in vitro proliferation method using MTT.[29] Briefly, 1.0×10^4 cells were plated in 96-well plates and incubated for 24 h to allow the cells to attach. The cells were exposed to serial concentrations of free PTX or PTX-loaded micelles at 37 °C for 48 h. At the end of incubation time, 20 μL of MTT solution was added and incubated for another 4 h at 37 °C, and then the medium was replaced with 200 μL of DMSO. The absorbance was read on a Sunrise absorbance microplate reader (Tecan) at dual wavelengths of 570 and 650 nm. The data reported represent the means of triplicate measurement; the standard errors of the mean were less than 15%. The cytotoxic effect of CSSA was also evaluated by the same method.

Cellular Uptake. Aliquots of A549 cells were exposed to free PTX or PTX-loaded micelles diluted in culture medium at 37 °C for 6 h (the PTX concentrations were 2.0, 10, and 20 μg/mL). At predetermined times, the cells were washed three times with ice-cold phosphate buffers (pH 7.2) to terminate the uptake and remove the free PTX or PTX-loaded micelles that was adsorbed on the cell membrane. The cells were collected by brief treatment with trypsin and diluted with methanol, followed by water-bath sonication under airproof conditions. Subsequently, the supernatant was obtained by centrifugation at 20 000 rpm for 10 min. The concentration of PTX in clean supernatant was determined by injection onto the HPLC system.

For investigating the intracellular distribution, drug-free micelles, PTX-loaded micelles, and chitosan oligosaccharides were further labeled with fluorescein isothiocyanate (FITC) via the reactive amino group of chitosan and the isothiocyanate group of FITC. Cells were seeded for 24 h into 24-well plates in 1 mL of RPMI 1640. Before uptake experiments, the medium in each well was replaced with 1 mL of fresh culture medium. The cells were incubated for 1 h with FITC-labeled micelles and were washed three times with ice-cold phosphate buffers (pH 7.2). The cells were observed by fluorescence microscopy (Olympus America, Melville, NY).

Fluorescence Quenching Studies. The aggregation number of stearic acid groups of CSSA was estimated by the steady-state fluorescence quenching method.[30] DPC was used as a fluorescence quencher for quenching of pyrene fluorescence. The sample solution

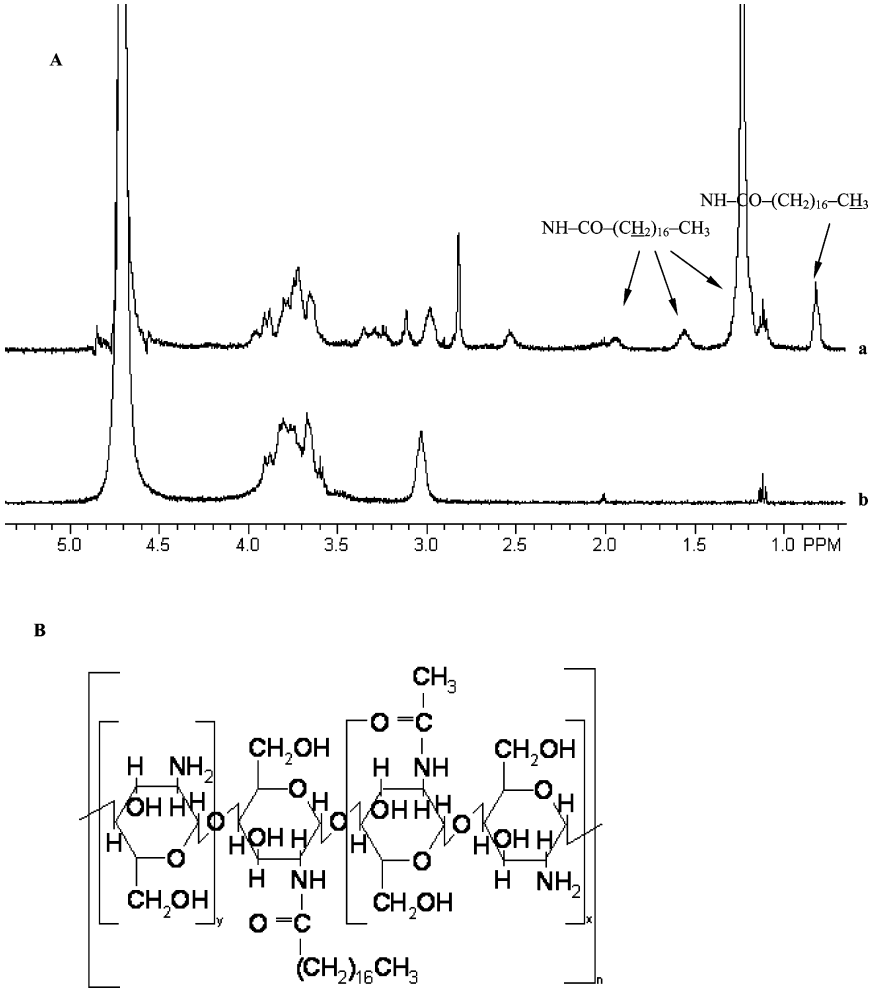

Figure 1. (A) ^{1}H NMR spectra of (b) chitosan oligosaccharide and (a) chitosan oligosaccharide derivative. (B) Possible chemical structure of stearate-grafted chitosan oligosaccharide.

containing settled pyrene (6.0×10^{-6} mol/L) and various DPC concentration was excited at 337 nm, and the emission spectra were at 390 nm. The slit openings for excitation and emission were 10.0 and 2.5 nm, respectively. The spectra were accumulated with an integration time of 5 s/nm.

3. Results and Discussion

CSSA with high DS was synthesized via reaction of the carboxyl group of stearic acid with the amine group of chitosan oligosaccharide in the presence of 1-ethyl-3-(3-dimethylaminopropyl)carbodiimide (EDC). EDC, as a coupling cross-linker,[31] first reacts with the carboxyl group of stearic acid to form an active ester intermediate. The formed intermediate can react with the primary amine of chitosan oligosaccharide to form an amide bond. The formation of amide bond between chitosan oligosaccharide and stearic acid was confirmed from ^{1}H NMR spectrum. By comparison with the spectrum of chitosan oligosaccharide (Figure 1A), the triple peaks at about 0.76 ppm in the ^{1}H NMR spectrum of CSSA (Figure 1B) were attributed to the methyl hydrogen of stearate group of CSSA [$-$NH$-$CO$-$(CH$_2$)$_{16}-$C$\underline{\text{H}}_3$]. The peaks at about 1.2, 1.5, and 1.9 ppm were attributed to the methylene hydrogen of stearate group of CSSA [$-$NH$-$CO$-$(C$\underline{\text{H}}_2$)$_{16}-$CH$_3$]. The results evidenced that the chitosan oligosaccharide derivative contained stearate groups. The DS of CSSA was about 34.7%. The yield of the synthesis was about 87%.

Figure 2 panels A and B show the size distribution of the micelles with 1.0 mg/mL CSSA concentration in pH 7.4 medium and the AFM image of drug-free micelles, respectively. The micelles had a close morphology to the discus as shown in the AMF image, and the observed micelle size coincided with that obtained from Zetasizer 3000 (mean volume size, 41 nm; polydispersity index, 0.146; ζ potential, 24 mV).

The micelle formation of the synthesized polymers was confirmed by fluorescence spectroscopy with pyrene as a probe. The I_1/I_3 ratio was used to determine the critical aggregation concentration (cac) of CSSA. Figure 2C shows I_1/I_3 of pyrene emission spectra (I_1, em = 374 nm; I_3, em = 386 nm) as a function of the concentration of CSSA and chitosan oligosaccharides. The cac values of CSSA and chitosan oligosaccharides were 5.59×10^{-3} and 0.39 mg/mL, respectively (Figure 2C). Compared with the unmodified chitosan oligosaccharides or low molecular weight surfactants, such as the critical micelle concentration (cmc) of 2.47 mg/mL for sodium dodecyl sulfate (SDS), CSSA have more stable self-aggregation in dilute condition.

The entrapment efficiency of PTX was about 89.5% and was stable for 3 months (about 84.0% after 3 months), which was calculated from the ratio of PTX in the micelles to the total drug amount used in the solution. The content of PTX in the micelles was about 6.5% (w/w). Figure 2D shows the accumulative PTX release profile. It is clear that the release rate of PTX from the micelles was retarded compared with free PTX

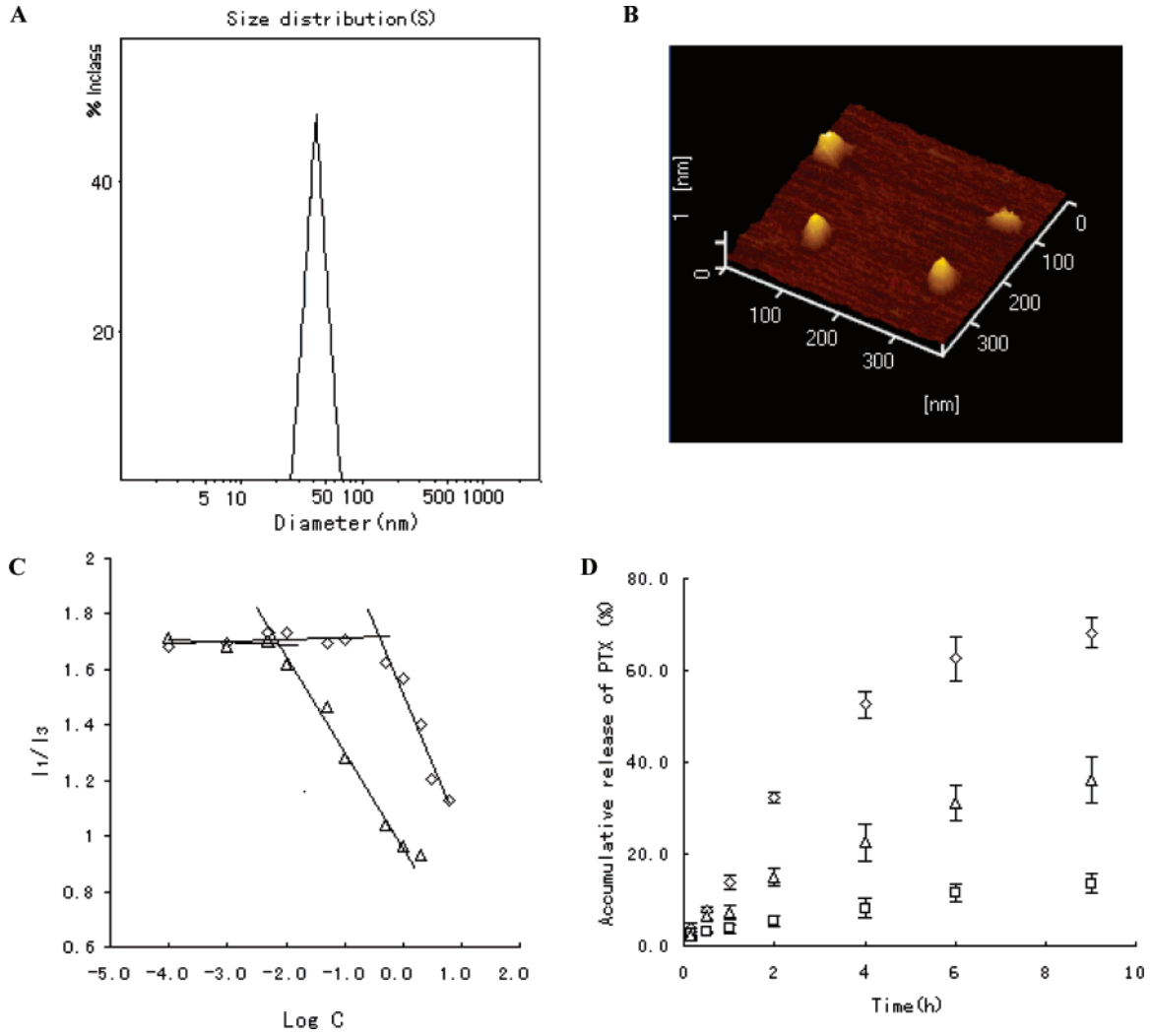

Figure 2. (A) Volume-weighted size distribution of drug-free micelles (1.0 mg/mL) in pH 7.4 medium. (B) AFM image of drug-free micelles. AFM was employed to observe the test micelle morphology and particle size. The sample was prepared by casting a dilute micelle solution on the mica surface, which was then in vacuo. (C) Variation of intensity ratio (I_1/I_3) vs concentration of CSSA (△) and chitosan oligosaccharide (◇). (D) Accumulative PTX release profile from micelles in dissolution media with different pH values containing 1 M sodium salicylate (mean + SD, $n = 3$). In the pH 7.4 dissolution medium, approximately 70% of PTX was diffused from dialysis bag after 9 h (◇), while 13% of PTX was released from the micelles after 9 h (□), showing the potential of the micelles as a sustained drug delivery system. Accumulative release of PTX from the micelles after 9 h was increased significantly with decreasing pH value of the dissolution medium. The accumulative release in the case of pH 6.2 dissolution medium (△) was 2.67-fold higher than that of pH 7.4 dissolution medium (□).

and sensitive to the pH of the dissolution medium. The release rate was enhanced with decreasing pH of dissolution medium, contributed to the increased size of the micelles and the weakened encapsulating ability in the medium with low pH (mean volume size, 240 nm; polydispersity index, 0.508; ζ potential, 46 mV). The reduction of pH allows protonation of the amino group on the chitosan oligosaccharide backbone. As a result, the electrostatic repulsion increases between CSSA molecules in the same micelle, and thus the micelle size, is augmented. Because the pH is about 7.4 in the extracellular environment of a tumor, drug release from the micelles is restrained, while the PTX release will be enhanced significantly due to the intracellular environment of pH 6.0∼6.5[32] when PTX-loaded micelles are internalized into cancer cell. Therefore, this pH-sensitive release behavior will favor the drug residence in the micelles during extracellular transport and promote intracellular delivery of the drug into its molecular target.

The cell inhibition results of PTX-loaded micelles and free PTX in HeLa and A549 cells are shown in Figure 3. There is a sharp discrimination in cell inhibition between free PTX and PTX-loaded micelles. The IC_{50} values of free PTX as control were 5.50 and 3.14 μg/mL for HeLa and A549, respectively, while the cytotoxicity of PTX-loaded micelles was enhanced significantly with IC_{50} values of 0.28 and 0.20 μg/mL for HeLa and A549, respectively. In contrast, the IC_{50} values of CSSA were 610 and 580 μg/mL for HeLa and A549, respectively, suggesting that CSSA showed low cytotoxicity against the cultured cells. The results indicated that higher cytotoxicity was obtained for PTX-loaded micelles compared with that of free PTX.

To explain the increased cytotoxicity of PTX-loaded micelles, the intracellular PTX concentration was determined by HPLC assay of collected A549 cells after the cells were incubated with different concentration of PTX-loaded micelles for different incubation times. As shown in Figure 4 A, the intracellular PTX amount was enhanced with increasing incubation time and encapsulated PTX concentration. Compared with free PTX, more PTX was found in the cells after PTX was encapsulated by the micelles at the same incubation condition. Even at the low drug concentration for PTX-loaded micelles (e.g., 2 μg/mL), a higher intracellular PTX amount was measured compared with that at the high drug concentration for free PTX (e.g., 20

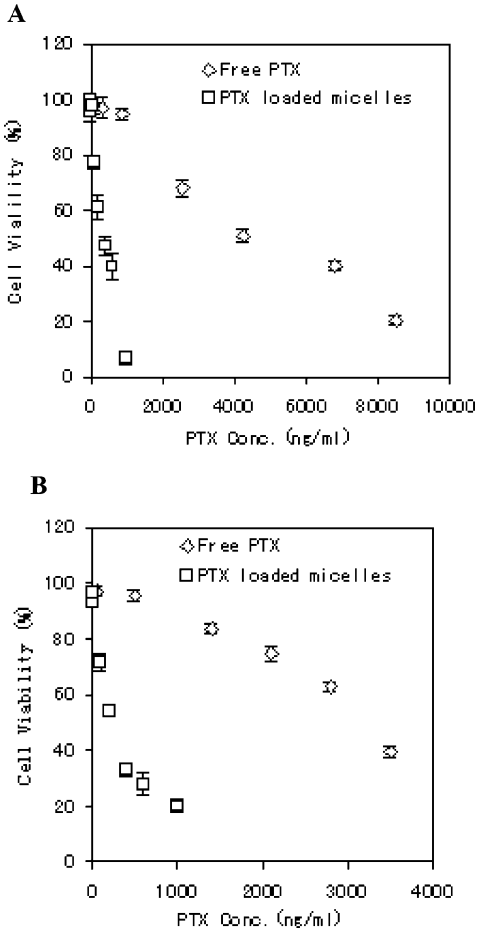

Figure 3. Cell viability variation vs PTX concentration. (A) HeLa and (B) A549 cells were incubated with (□) PTX-loaded micelles and (◇) free PTX for 48 h (mean ± SD, $n = 3$).

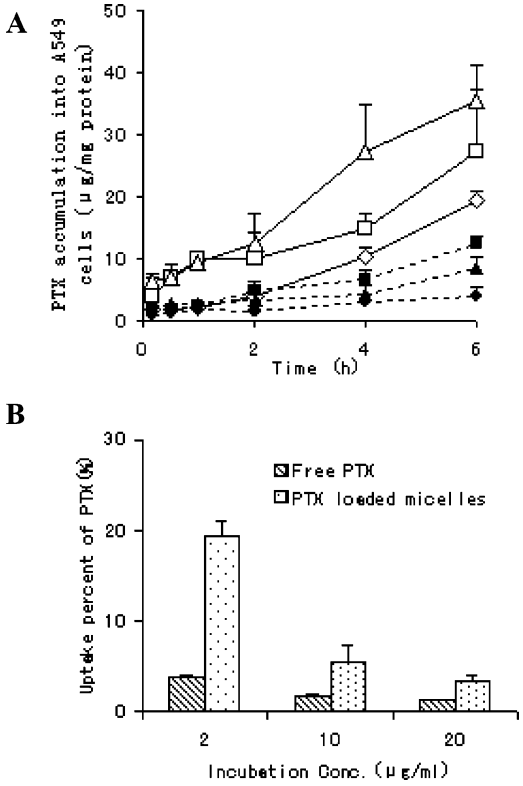

Figure 4. (A) Intracellular uptake of PTX to A549 cells incubated with free PTX or PTX-loaded micelles (mean ± SD, $n = 3$). The incubation concentration of the drug is (◆) 2.0, (▲) 10, and (■) 20 μg/mL for free PTX and (◇) 2.0, (□) 10, and (△) 20 μg/mL for PTX-loaded micelles. (B) PTX uptake percentage change versus incubation concentration at the 6 h incubation time for PTX-loaded micelles and free PTX (mean ± SD, $n = 3$).

μg/mL). After 6 h of incubation, the internalization of micelle-loaded PTX into the cells was 4.97-, 3.23-, and 2.85-fold higher than that of free PTX at drug concentrations of 2.0, 10, and 20 μg/mL, respectively (Figure 4B). These results confirmed that intracellular delivery of PTX had been enhanced significantly via the mediated transport by the micelles. As a result, PTX-loaded micelles can obtain higher cell cytotoxicity compared with free PTX.

Figure 5 shows the fluorescence images after the FITC-labeled drug-free micelles, PTX-loaded micelles, and self-aggregated chitosan oligosaccharides were incubated with A549 cells for 1 h. Strong green fluorescence in cells was observed after the treatment with micelles (Figure 5A), and the observed fluorescence intensity was enhanced significantly for longer incubation times, indicating excellent internalization of the micelles. The micelle seemed to possess rapider cellular uptake comparing with liposomes and solid lipid nanoparticles (unpublished data). However, self-aggregations of chitosan oligosaccharides presented poor internalization into cells under the same incubation conditions (Figure 5C), even for longer incubation times. Most self-aggregations adhered on the cell surface, which seemed to penetrate through the plasma membrane with difficulty. It was also obvious that observed green fluorescence was mostly distributed in cytoplasm (Figure 5A,B), suggesting that micelles possess the cytoplasm-targeting localization and delivery. Furthermore, the property of cytoplasm-targeting was not changed after PTX was loaded into the micelles (Figure 5B). It means that PTX can be transported into cells and subsequently accumulate in cytoplasm, as the molecular target site of PTX, via the encapsulation of the micelles.

Why can the micelles enhance intracellular delivery of PTX? It is attributable to the excellent internalization of the micelles into cells, attributed to their components and special spatial structure. Chitosan has demonstrated its potential as a drug carrier and a membrane perturbant for subsequent drug delivery to cells,[33] and it can directly perturb the organization of the hydrophobic inner core of the dipalmitoyl-*sn*-glycero-3-phosphocholine (DPPC) bilayer,[34] as an in vitro simulative biomembrane. Chitosan modified by alkyl chains could adhere to the biomembrane and tightly enfold the liposome anchoring their alkyl chains.[35] Furthermore, Liu et al.[36] have demonstrated that chitosans and alkylated chitosans can cause the fusion of DPPC multilamellar vesicles as well as membrane destabilization. The perturbation effect induced by alkylated chitosans is more evident due to the hydrophobic interaction. It is proposed that, upon elongating the alkyl side chain, the higher transfection efficiency of alkylated chitosans, as a gene vector, was obtained, which is attributed to the increasing entry into cells facilitated by hydrophobic interactions.[36] On the other hand, lipid modification of protein plays a key role in its association with biomembrane. A variety of proteins are targeted into membrane rafts, mostly by means of covalent lipid modifications. For attachment to the membrane and localization in membrane lipid domains, proteins require at least a second fatty acyl substitution.[37,38]

Figure 6 shows the possible structure of a micelle. Chitosans with protonated amines form the hydrophilic shell, and most of the stearic chains are assembled to become a hydrophobic

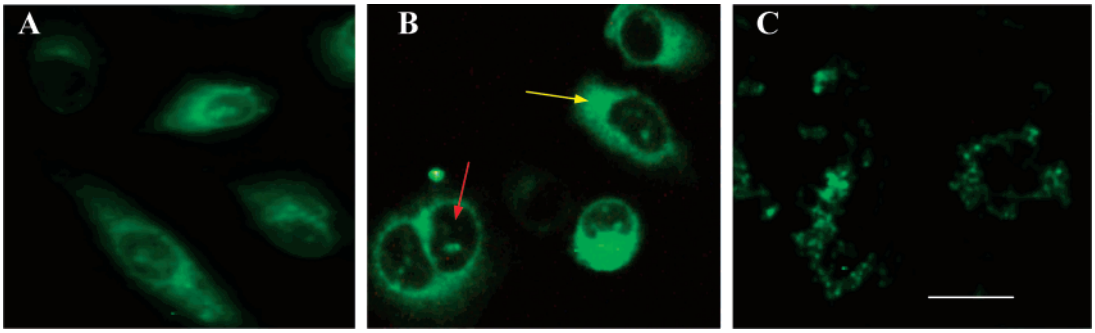

Figure 5. Uptake of (A) drug-free micelles, (B) PTX-loaded micelles, and (C) self-aggregations of chitosan oligosaccharides into A549 cells. Cells were incubated for 1 h with material (chitosan oligosaccharide) concentration of 0.5 mg/mL in order to obtain the self-aggregation. PTX loaded micelles and drug-free micelles also keep the same concentration in order to obtain parallel comparison. Red arrow, nucleus; Yellow arrow, cytoplasm. Bar, 30 μm.

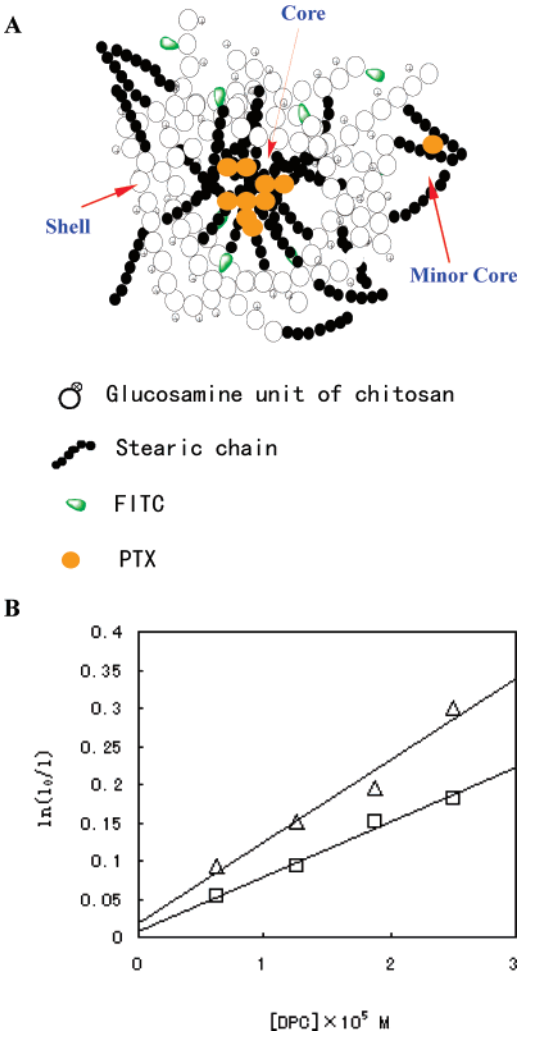

Figure 6. (A) Possible structure of a micelle in the aqueous medium. (B) Plots of ln (I_0/I) of pyrene fluorescence vs DPC concentration in the presence of the micelles. The concentration of CSSA in pH 7.4 aqueous medium was (△) 0.5 and (□) 1.0 mg/mL.

core. Some stearic chains are assembled to form the "minor cores" (hydrophobic microdomains) near the surface of the shell duo to the stereo resistance effect from the shell. To identify the microscopic structure of self-aggregates, the aggregation number of stearic acid groups was estimated by the steady-state fluorescence quenching method. This method has been applied to determine the aggregation number of micelles consisting of low-molecular-weight surfactants[39] or polymeric amphiphiles.[40] The steady-state quenching data fit in quenching kinetics (eq 1):[40,41]

$$\ln (I_0/I) = [Q]/[M] \quad (1)$$

where I_0 and I are the fluorescence emission intensity in the absence and presence of a quencher, respectively, [Q] is the concentration of the quencher, and [M] is the concentration of hydrophobic microdomains in self-aggregates. The results are shown in Figure 6b. Thus, the aggregation number of stearic acid groups per hydrophobic microdomain was 7.09 ± 0.77, calculated by eq 2. The number of hydrophobic microdomains that may be formed by one CSSA chain was 8.11 ± 0.84, calculated from the ratio of the total number of stearic acid groups in one CSSA chain to N_{SA}:

$$N_{SA} = [\text{stearic acid}]/[M] \quad (2)$$

Therefore, the surface of the micelles may possess more hydrophobic domains compared with the conventional polymer micelles, thus resulting in partial hydrophobicity near the micelle surface. There are several hypotheses to explain the mechanism of internalization of the micelles into cells: The glycolipid-like components of the micelles promote the affinity between the micelle and the cellular membrane. Furthermore, the positive charge of the micellar shell allows the micelles to bind to the cellular membrane via electrostatic interaction with negatively charged components in cellular membrane, and then the hydrophobic "minor core" near the surface of the micellar shell may play an important role in internalization of the micelles. The "minor cores" can insert into the celluar membrane, exerting hydrophobic interactions with membrane components, resulting in membrane perturbation and fusion, thus facilitating endocytosis of the micelles. Subsequently, the micelles can escape rapidly from the lysosome into the cytosol by the same means. Self-aggregations of chitosan oligosaccharides lacked sufficiently hydrophobic domains near their surface and thus presented poor cellular uptake.

4. Conclusion

In this work, polymeric micelles with glycolipid-like structure and about 40 nm diameter are prepared by self-aggregation from stearate-grafted chitosan oligosaccharides in aqueous medium. The micelles, with high DS, present specific spatial structure with multiple hydrophobic minor cores and thus obtain excellent internalization into cancer cells and accumulation in cytoplasm. Furthermore, the micelles showed pH-sensitive properties, thus favoring intracellular delivery of encapsulated drug. The cell

cytotoxicity of PTX loaded in micelles was improved sharply and contributed to the increased intracellular delivery of drug. The present micelles are a promising carrier candidate for targeted therapy of antitumor drugs with the molecule target in cytoplasm.

Acknowledgment. We appreciate the financial support of the National Nature Science Foundation of China under Contract 30472101 and the Nature Science Foundation of Zhejiang province under Contract M303817.

References and Notes

(1) Matsumura, Y.; Maeda, H. *Cancer Res.* **1986**, *46*, 6387−6392.
(2) Papahadjopoulos, D.; Allen, T. M.; Gabizon, A. *Proc. Natl. Acad. Sci. U.S.A.* **1991**, *88*, 11460−11464.
(3) Fabrizio, M.; François, L. *Drug Discovery Today* **2004**, *9*, 219−228.
(4) Cemazar, M.; Pavlin, D.; Kranjc, S.; Grosel, A.; Mesojednik, S.; Sersa, G. *Curr. Drug Delivery* **2006**, *3*, 77−81.
(5) Davidson, B. L.; Breakefield, X. O. *Nat. Rev. Neurosci.* **2003**, *4*, 353−364.
(6) Ramachandran, S.; Quist, A. P.; Kumar, S.; Lal, R. *Langmuir* **2006**, *22*, 8156−8162.
(7) Huth, U. S.; Schubert, R.; Peschka-Suss, R. *J. Controlled Release* **2006**, *110*, 490−504.
(8) Torchilin, V. P. *J. Controlled Release* **2001**, *73*, 137−172.
(9) Leamon, C. P.; Low, P. S. *Proc. Natl. Acad. Sci. U.S.A.* **1991**, *88*, 5572−5576.
(10) Jang, J. S.; Kim, S. Y.; Lee, S. B.; Kim, K. O.; Han, J. S.; Lee, Y. M. *J. Controlled Release* **2006**, *113*, 173−182.
(11) Park, E. K.; Kim, S. Y.; Lee, S. B.; Lee, Y. M. *J. Controlled Release* **2005**, *109*, 158−168.
(12) Park, E. K.; Lee, S. B.; Lee, Y. M. *Biomaterials* **2005**, *26*, 1053−1061.
(13) Soppimath, K. S.; Aminabhavi, T. M.; Kulkarni, A. R.; Rudzinski, W. E. *J. Controlled Release* **2001**, *70*, 1−20.
(14) Silvia, M.; Schuchman, H. E.; Vladimir, R. M. *Mol. Ther.* **2006**, *13*, 135−141.
(15) Qu, X.; Khutoryanskiy, V. V.; Stewart, A.; Rahman, S.; Papahadjopoulos-Sternberg, B.; Dufes, C.; McCarthy, D.; Wilson, C. G.; Lyons, R.; Carter, K. C.; Schazlein, A.; Uchegbu, I. F. *Biomacromolecules* **2006**, *7*, 3452−3459.
(16) Feng, H.; Dong, C.-M. *Biomacromolecules* **2006**, *7*, 3069−3075.
(17) Jiang, G. B.; Quan, D.; Liao, K.; Wang, H. *Mol. Pharmaceutics* **2006**, *3*, 152−160.
(18) Lee, K. Y.; Jo, W. H. *Micromolecules* **1998**, *31*, 378−383.
(19) Felgner, J. H.; Kumar, R.; Sridhar, C. N.; Wheeler, C. J.; Tsai, Y. J.; Border, R.; Ramsey, P.; Martin, M.; Felgner, P. L. *J. Biol. Chem.* **1994**, *269*, 2550−2561.
(20) Antonella, M.; Roberta, C.; Claudia, B.; Ludovica, G.; Maria, R. G. *Int. J. Pharm.* **2000**, *210*, 61−67.
(21) Hu, F. Q.; Ren, G. F.; Yuan, H.; Du, Y. Z.; Zeng, S. *Colloids Surf., B* **2006**, *50*, 97−103.
(22) Hu, F. Q.; Zhao, M. D.; Yuan, H.; You, J.; Du, Y. Z.; Zeng, S. *Int. J. Pharm.* **2006**, *315*, 158−166.
(23) Schiff, P.; Fant, J.; Horwitz, S. B. *Nature* **1979**, *277*, 665−667.
(24) Schiff, P.; Horwitz, S. B. *Proc. Natl. Acad. Sci. U.S.A.* **1980**, *77*, 1561−1565.
(25) Rowinsky, E. K.; Donehower, R. C.; Jones, R. J.; Tucker, R. W. *Cancer Res.* **1988**, *48*, 4093−4100.
(26) Andres, B. S.; Martina, E. K. *J. Controlled Release* **1998**, *50*, 215−223.
(27) Lee, E. S.; Na, K.; Bae, Y. H. *J. Controlled Release* **2003**, *91*, 103−13.
(28) Cho, Y. W.; Lee, J.; Lee, S. C.; Hu, K. M.; Park, K. *J. Controlled Release* **2004**, *97*, 249−257.
(29) Mosmann, T. *J. Immunol. Methods* **1983**, *65*, 55−63.
(30) Lee, K. Y.; Jo, W. H. *Macromolecules* **1998**, *31*, 378−383.
(31) Hermanson, G. T.; Mallia, A. K.; Smith, P. K. Academic Press: San Diego, CA, 1992.
(32) Maxfield, F. R.; McGraw, T. E. *Mol. Cell. Biol.* **2004**, *5*, 121−132.
(33) Fang, N.; Chan, V. *Biomacromolecules* **2003**, *4*, 1596−1604.
(34) Fang, N.; Chan, V.; Mao, H. Q.; Leong, K. W. *Biomacromolecules* **2001**, *2*, 1161−1168.
(35) Nonaka, K. I.; Kazama, S.; Goto, A.; Fukuda, H.; Yoshioka, H. *J. Colloid Interface Sci.* **2002**, *246*, 288−295.
(36) Liu, W. G.; Zhang, X.; Sun, S. *Bioconjugate Chem.* **2003**, *14*, 782−789.
(37) Casey, P. J. *Science* **1995**, *268*, 221−225.
(38) Resh, M. D. *Biochim. Biophys. Acta* **1999**, *1451*, 1−16.
(39) Ueno, M.; Kimoto, Y.; Ikeda, Y.; Momose, H.; Zana, R. J. *J. Colloid Interface Sci.* 1**987**, *117*, 179−186.
(40) Chu, D. Y.; Thomas, J. K. *Macromolecules* **1987**, *20*, 2133−2138.
(41) Turro, N. J.; Yekta, A. J. *J. Am. Chem. Soc.* **1978**, *100*, 5951−5952.

BM070365C